Bound states in the continuum in quantum dot pairs

Gonzalo Ordonez and Kyungsun Na
Center for Studies in Statistical Mechanics and Complex Systems, The University of Texas at Austin, Austin, TX 78712 USA

Sungyun Kim
Max-Planck Institute for Physics of Complex Systems Noethnizter Str. 38, 01187 Dresden Germany

It is shown that for two open quantum dots connected by a wire, "bound states in the continuum" of a single electron are formed at nearly periodic distances between the dots. This is due to Fabry-Pérot interference between quasi-bound states in each dot. The bound states are non-local, describing the electron trapped in both dots at the same time. Theoretical and numerical results show that trapped states exist even if the wire connecting the dots is relatively long.

PACS numbers: 03.65.-w, 73.23.-b, 73.63.-b

Ever since von Neumann and Wigner [1] proposed that certain type of oscillating attractive potentials could produce isolated bound states with energies within the continuum [2], a number of studies have reported the existence of "bound states in the continuum" (BIC) that can exist above the continuum minimum. Fonda and Newton discussed BIC in a system of two coupled square-well potentials using resonance scattering theory [3]. Friedrich and Wintgen found BIC in systems of coupled Coulombic channels, such as the hydrogen atom in a uniform magnetic field [4]. Positive energy bound states in superlattice structures with a single impurity potential [5] or a single defect stub [6] have been reported.

Existence of BIC has been theoretically demonstrated as well in a pair of quantum dots coupled to reservoirs [7, 8]. The pair of dots is regarded as a "molecule" with discrete energy levels. As far as we know, until now there is no experimental realization of BIC in quantum dots.

Here we present a quantum dot system where BIC are formed due to Fabry-Pérot interference between quasi-bound states of each dot. In our system, the dots are two-dimensional square cavities connected to a lead as shown in Fig. 1. In contrast to Refs. [7, 8], instead of one "molecule" we have two separate dots that can be far apart. Therefore we study quite a different regime of electron transport between dots.

The dots and the lead make a two dimensional electron waveguide. Such waveguides can be formed at a GaAs/AlGaAs interface [9]. Electron wave guides may also be formed using carbon nanotubes, where Fabry-Pérot interference for electron wave functions has been demonstrated experimentally [10]. In this paper we will focus on semiconductor wave guides.

The lead in Fig. 1 is an infinite quasi-one-dimensional wire, where electrons have a continuous spectrum of energy. Due to the lateral confinement in the wire, the spectrum has a minimum energy that allows propagation along the wire. If there is a single dot, an electron inside the dot with energy below the minimum will form bound states. In contrast, an electron with energy above

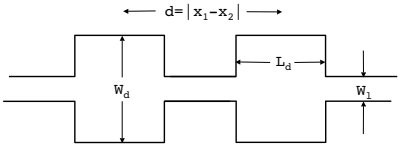

FIG. 1: Quantum dot pair

the minimum will form quasi-bound states with finite life-time, where the electron escapes the dot through the leads. Bound states and quasi-bound states are associated with real and complex poles of the S-matrix [11].

For the double-dot, the electron states are much more varied. In this study, we focus on the interplay between the quasi-bound states formed in each dot. We find BIC appear at nearly periodic distances between the dots.

Theoretical model. We use the single-electron Hamiltonian

$$H = -\frac{\hbar^2}{2m_e^*}\left(\frac{\partial^2}{\partial x^2}+\frac{\partial^2}{\partial y^2}\right) \tag{1}$$

with vanishing wavefunctions at the boundaries. The effective mass is $m_e^* = 0.05m_e$, where m_e is the mass of the free electron. We assume the two dots are identical. To analyze this Hamiltonian, we decompose the system into two independent closed dots and the lead [14]. The wavefunctions inside the dots are denoted by $|m,n\rangle_i$, where $i = 1, 2$ labels the dots and m, n are positive integers representing the horizontal and vertical wave numbers. The wavefunctions in the leads are denoted by $|k, j\rangle$ where k is the horizontal wave number (real) and j the vertical wave number (positive integer). The energies of the wavefunctions in either dot and the lead are respectively

$$\begin{aligned} E_d(m,n) &= \frac{\hbar^2}{2m_e^*}\left[\left(\frac{m\pi}{L_d}\right)^2+\left(\frac{n\pi}{W_d}\right)^2\right] \\ E_l(k,j) &= \frac{\hbar^2}{2m_e^*}\left[k^2+\left(\frac{j\pi}{W_l}\right)^2\right] \end{aligned} \tag{2}$$

The minimum energy for propagation along the lead is $E_l(0,1)$. We consider an electron with low energy narrowly centered around, $E_d^0 = E_d(m_0, n_0)$. We assume that $E_l(0,1) < E_d^0 < E_l(0,2)$. The electron may propagate through the first mode of the lead, but not through the higher ($j > 1$) modes. In our theoretical model, we neglect the $j > 1$ modes, which are evanescent, and keep only the $j = 1$ mode. Henceforth we omit the $j = 1$ index, e.g., $E_l(k) = E_l(k, 1)$.

We will rewrite the Hamiltonian using the dot and lead basis states. With $|i\rangle = |m_0, n_0\rangle_i$, we define the dot and lead projectors

$$P_d = \sum_{i=1}^{2} |i\rangle\langle i|, \quad P_l = \int_{-\infty}^{\infty} dk\, |k\rangle\langle k| \tag{3}$$

To make the basis states orthogonal, we introduce the modified lead states

$$\begin{aligned} |\psi_k\rangle &= |k\rangle - RP_d(P_dRP_d)^{-1}|k\rangle, \\ R &= \frac{1}{E_l(k) - P_lHP_l + i0} \end{aligned} \tag{4}$$

that satisfy $\langle i|\psi_k\rangle = 0$ and $\langle\psi_{k'}|H|\psi_k\rangle = E_l(k)\delta(k-k')$. The following approximate Hamiltonian is obtained

$$\begin{aligned} H &\approx E_d^0\left[|1\rangle\langle 1| + |2\rangle\langle 2|\right] + \int_{-\infty}^{\infty} dk E_l(k)|\psi_k\rangle\langle\psi_k| \\ &+ \left[\int_{-\infty}^{\infty} dk \sum_{i=1}^{2} V_i(k)|i\rangle\langle\psi_k| + \text{H.c.}\right] \end{aligned} \tag{5}$$

The terms $V_i(k) = \langle i|H|\psi_k\rangle$ represent the amplitude of a transition of the electron from the lead to the dots or vice versa. For dots centered at $x = x_1$ and $x = x_2$, they have the form

$$V_{1,2}(k) = v_k e^{ikx_{1,2}} + u_k e^{ikx_{2,1}} \tag{6}$$

In Ref. [12] the appearance of BIC for a one-dimensional two-atom system was considered (see also [13]). That system has a Hamiltonian similar to (5). Hence to analyze theoretically the double-dot waveguide we follow an approach similar to the approach described in Ref. [12].

To construct eigenstates of the Hamiltonian (5) we start with the symmetric and anti-symmetric states

$$|\pm\rangle = \left(|1\rangle \pm |2\rangle\right)/\sqrt{2} \tag{7}$$

From Eq. (7) we obtain symmetric and anti-symmetric eigenstates with complex energy eigenvalues $z_\pm$ respectively [12], which are poles of the S-matrix. For $t > 0$ we take the eigenvalues with negative imaginary part. They are solutions of the integral equation

$$z_\pm = E_d^0 + 2\int_0^\infty dk \frac{|u_k \pm v_k|^2}{(z_\pm - E_l(k))^+}(1 \pm \cos kd) \tag{8}$$

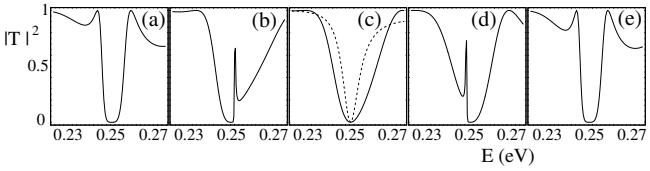

FIG. 2: Transmission probability, $|T|^2$, versus energy, E, for the double-dot waveguide with $W_d = 2$, $L_d = 2$, $W_l = 1$, and (a) $d = 5.25$, (b) $d = 5.5$, (c) $d = 5.60$, (d) $d = 5.70$, and (e) $d = 5.90$. The dashed line in (c) is the transmission probability for the single-dot waveguide.

closest to the real axis. Here $d = |x_2 - x_1|$ is the distance between the dots. The + superscript means analytic continuation from the upper to the lower half-plane of $z_\pm$. As the distance d is varied, the poles $z_\pm$ move in the complex plane. At certain distances $d_\pm$ the imaginary part of $z_\pm$ vanishes [12]. This happens when $1 \pm \cos kd_\pm = 0$ for $E_l(k) = z_\pm$. These conditions give

$$d_\pm = \frac{2n + (1 \pm 1)/2}{\sqrt{2m_e^*(z_\pm - E_l(0))}}\pi\hbar \tag{9}$$

with n integer. Replacing $d = d_\pm$ in Eq. (8) we obtain real solutions for $z_\pm$, which implies the existence of BIC. This effect is essentially due to Fabry-Pérot interference between the wave functions escaping from each dot. As shown in Ref. [12], BIC appear even for large $d_\pm$. Thus, in principle, the wire connecting the dots can be relatively long and still allow BIC. Note that $d_\pm$ is a nonlinear function of n. Strictly speaking the distances $d_\pm$ are not regularly spaced.

In the following we verify the existence of BIC using a more accurate description of the system.

Computational results. We have computed the energy eigenstates for the lowest propagating mode in the double-dot waveguide as a function of energy and the distance between the two dots using the boundary integral method [11, 15]. The eigenstates are built out of local propagating and evanescent modes in the leads and dots and are composed of incoming, $\psi^-(x,y)$, and outgoing, $\psi^+(x,y)$, states

$$\psi(x,y) = \psi^-(x,y) + S(E)\psi^+(x,y), \tag{10}$$

where the scattering amplitude, $S(E)$, is composed of reflection and transmission coefficients. The unit of length is the width of the lead, $W_l = 1$, which corresponds to $100\mathring{A}$. The width and length of each dot are $W_d = 2$ and $L_d = 2$, respectively. These parameters satisfy the conditions of validity of the theoretical model, and we will use them as an example.

We have computed the transmission probability, $|T|^2$, for the lowest propagating mode as a function of energy for the double-dot waveguide in Fig. 2. As we vary the distance between the two dots, the transmission profiles

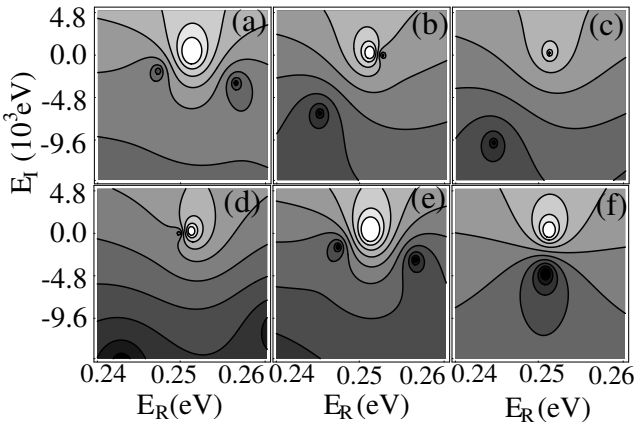

FIG. 3: Transmission amplitude, $T(E)$, in the complex energy plane, $E = E_R + iE_I$, for the double-dot waveguide with $W_d = 2$, $L_d = 2$, $W_l = 1$, and (a) $d = 5.25$, (b) $d = 5.5$, (c) $d = 5.60$, (d) $d = 5.70$, and (e) $d = 5.90$. The transmission amplitude in the complex energy plane for the single-dot waveguide is in (f). The dark regions indicate the positions of the poles and the bright region indicates the position of the transmission zero.

change near the resonance energy region $E_d^0 = 0.25eV$. There are sharp peaks in the transmission profiles on either side of the resonance energy regions in Figs. 2 (b) and (d). There is a broad transmission profile with $d = 5.60$ in Fig. 2 (c). For comparison, the transmission probability for the single-dot waveguide is shown in Fig. 2 (c) as a dotted line. The transmission zero profile shows a wider dip for the double-dot waveguide as compared with that of the single-dot waveguide. We will see later that the BIC is formed when the distance between the two dots is $d = 5.60$, as well as at other distances nearly regularly spaced. These features are associated with the presence of two poles in the complex energy plane, which affect the dynamics of the electron in the double-dot waveguide.

The transmission zeros in Fig. 2 are associated with the poles of $T(E)$ in the complex energy plane. The transmission amplitude in the complex energy plane has a branch cut starting from the lower edge of the continuum and extending along the positive energy axis and has poles at energies $z = \omega - i\gamma$. These poles give rise to the transmission zeros on the positive real axis [11, 16].

The locations of the poles in the complex energy plane for the double-dot waveguide are shown in Figure 3. As we increase the distance between the two dots, the pole located on the right-hand side in Fig. 3 (a) approaches the real axis. The pole disappears into the real axis and produces a zero value of γ at the distance, $d = 5.60$, in Fig. 3 (c). This implies the formation of a BIC with infinite life-time. The pole on the left-hand side in Fig. 3 (a) moves away from the real axis and attains large decay rate γ, accordingly. As the distance between the dots is further increased, the pole on the real axis in Fig. 3 (c) emerges out of the transmission zero and recedes from the real axis (Fig. 3 (d)). If we continue to increase d, the pole on the right-hand side in Fig. 3 (e) approaches the real axis and makes a transit through the transmission zero at $d = 6.28$ (not shown).

d (c)	2.30	2.96	3.61	4.28	4.95	5.60	6.28	..	47.9	48.5	49.2
d (t)	2.67	3.33	4.00	4.67	5.33	6.00	6.67	..	48.0	48.7	49.3

TABLE I: Computational (c) and theoretical (t) values of inter-dot distance at which BIC appear.

The wavefunctions inside the two dots for the real energy states associated with the right-hand side and left-hand side poles in Fig. 3 (a) show symmetric and anti-symmetric structures, respectively. These wavefunctions are similar to the symmetric and anti-symmetric combinations of the eigenstates of the two closed dots,

$$\psi_\pm(x,y) = \frac{1}{\sqrt{2}}(\sin(2\pi(x-x_1)/L_d)\cos(3\pi y/W_d)\chi_1 \pm \sin(2\pi(x-x_2)/L_d)\cos(3\pi y/W_d)\chi_2) \quad (11)$$

where $\chi_i = 1$ inside dot i and $\chi_i = 0$ outside. Eq. (11) corresponds to Eq. (7). Each complex pole keeps its symmetric or anti-symmetric feature as it migrates throughout the complex energy plane, as we vary the distance between the two dots. The BIC appearing at $d = 5.6$ is symmetric and at $d = 6.28$, anti-symmetric.

BIC reappear in a nearly periodic fashion as the distance between the two dots is varied (see Table I) . This agrees with the existence of real solutions of Eq. (8) with Eq. (9) for different values of n. For example, solutions of Eq. (8) for $n = 4$ and $n = 5$ give $d_+ = 6$ and $d_- = 6.67$, respectively. The difference between the theoretical and computational values of d in Table I is likely due to the cutoff of $j > 1$ modes in the theoretical model [14]. However the theoretical spacing between consecutive distances is in good agreement with the computational results. We have found BIC for distances of up to $d \approx 50$, which means that these states may be quite de-localized.

In Fig. 3 each of the poles with either symmetric or anti-symmetric identity makes a counter-clockwise circulation that passes through the transmission zero on the real axis as vary the distance between dots. It has been known that the double or multiple poles induced by a laser in an atom coalesce to form an exceptional point or repel each other to form an avoided crossing [17–19]. In contrast, the poles of the double-dot waveguide make a circular motion and do not approach or repel each other.

One of the important features of an electron waveguide is that the energy spectrum of the electrons is continuous. This means that the electron waveguides fall in the class of unstable systems. An electron in the dot with wavelength smaller than the critical wavelength for

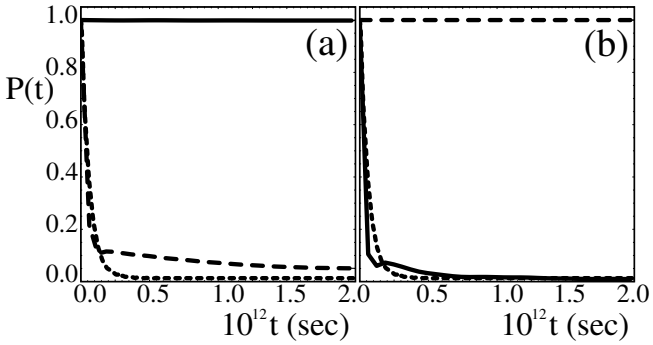

FIG. 4: The survival probability, $P(t) = |A(t)|^2$, versus time, t, for the states prepared symmetrically or anti-symmetrically inside the two dots at $t = 0$. The distances between the two dots are (a) $d = 5.60$ and (b) $d = 6.28$. The dotted line shows the survival probability of a state in the single-dot waveguide in (a) and (b). The solid line displays the survival probability of a state prepared symmetrically and the dashed line displays the survival probability of a state prepared anti-symmetrically.

propagation along the lead, will ultimately decay (escape through the leads). However, in our study, we have shown that for special distances d the electron in the double-dot waveguide can be trapped in a non-decaying state with infinite life-time, forming BIC.

The survival probabilities of an electron placed in the waveguide dots can be calculated using the scattering states of the double-dot waveguide. The survival probability can be written as $P_\psi(t) = |A_\psi(t)|^2$, where $A_\psi(t)$ is the survival amplitude,

$$A_\psi(t) = \langle\psi|\mathrm{e}^{-i\hat{H}t/\hbar}|\psi\rangle = \int_0^\infty dE|\langle\psi|E\rangle|^2\mathrm{e}^{-iEt/\hbar}. \quad (12)$$

We choose as initial state $|\psi\rangle$, the symmetric or anti-symmetric combinations of the eigenstates of the two closed dots in Eq. (11), with no probability amplitude outside the dots. In order to solve Eq. (12) numerically, we discretize the energy eigenstates, $|E\rangle$, residing in the continuum.

In Fig. 4, we plot the survival probability, $P(t) = |A(t)|^2$, versus time, t for the states prepared symmetrically or anti-symmetrically inside the two dots at $t = 0$. The distances between the two dots are $d = 5.60$ and $d = 6.28$ for Figs. 4 (a) and (b), respectively.

With this arrangement, one of the complex poles has a vanishing imaginary part, $\gamma \to 0$, and gives rise to an infinite life-time. The results show that the symmetrically (anti-symmetrically) arranged state does not decay over time for the cases with $d = 5.60$ (6.28). On the other hand, the anti-symmetric (symmetric) state decays quickly. The dotted line in Fig. 4 shows the survival probability of the state, $\psi = \sin(2\pi x/L_d)\cos(3\pi y/D_d)$, in the single-dot waveguide.

In conclusion, we have proved that there can be BIC in double-dot electron waveguides with specially arranged geometry. These can be used as a quantum information storing device. Pairs of electrons with opposite spins may form de-localized, entangled states. Also, we could make the electron flow or get trapped inside the dots by controlling the size of the one of the dots. This feature might be useful in a circuit device. The existence of BIC may be verified experimentally using actual electron waveguides. Alternative experimental setups are electromagnetic waveguides, which are described by a similar model, and super lattices with two impurities [20]. Three-dimensional electron wave guides analogous to Fig. 1 may be constructed using nanotubes [10].

We thank Professors T. Petrosky, L. Reichl, S. Tanaka, R. Walser and P. Valanju for helpful comments and suggestions. We acknowledge the Engineering Research Program of the Office of Basic Energy Sciences at the U.S. Department of Energy, Grant No DE-FG03-94ER14465 and U.S. Navy Office of Naval Research, Grant No. N00014-03-1-0639 for partial support of this work.

[1] J. von Neumann and E. Wigner, Phys. Z. **30**, 465 (1929).
[2] F. H. Stillinger and D. R. Herrick, Phys. Rev. A **11** 446(1975); B. Gazdy, Phys. Lett. **61A** 89 (1977).
[3] L. Fonda and R. G. Newton, Ann. Phys. (N.Y.) **10** 490 (1960).
[4] H. Friedrich and D. Wintgen, Phys. Rev. A **31** 3964 (1985).
[5] F. Capasso et al, Nature **358** 565 (1992).
[6] P. S. Deo and A. M. Jayannavar, Phys. Rev. B **50** 11629 (1994).
[7] M. L. Ladrón de Guevara, F. Claro and P. A. Orellana, Phys. Rev. B **67** 195335 (2003).
[8] I. Rotter and A. Sadreev, Phys. Rev. E **71** 046204 (2005).
[9] S. Datta, *Electronic Transport in Mesoscopic Systems* (Cambridge University Press, Cambridge, 1995).
[10] W. Liang et al., Nature **411**, 665 (2001); C. White and T. Todorov, Nature **411**, 649 (2001).
[11] K. Na and L.E. Reichl, J. Stat. Phys. **92** 519 (1998).
[12] G. Ordonez and S. Kim, Phys. Rev. A **70**, 032702 (2004).
[13] G. Sudarshan, in *Field theory, quantization and statistical physics,* edited by E. Tirapegui (D. Reidel Publishing Company, 1981), p. 237.
[14] T. Petrosky and S. Subbiah, Physica E **19**, 230 (2003); S. Subbiah, Dissertation, The University of Texas at Austin (2000).
[15] F.R. Frohne, M.J. McLennan, and S. Datta, J. Appl. Phys. **66** 2699 (1989).
[16] K. Na and L.E. Reichl, Phys. Rev. B **59** 13073 (1999).
[17] O. Latinne et al., Phys. Rev. Lett. **74** 46 (1995).
[18] N.J. Kylstra and C. J. Joachain, Phys. Rev. A **57** 412 (1998).
[19] A. I. Magunov, I. Rotter, and S. I. Strakhova, J. Phys. B : At. Mol. Opt. Phys. **34** 29 (2001).
[20] G. Ordonez, S. Tanaka, and T. Petrosky, unpublished.